

Effect of a Magneto-hydrodynamic Natural Convection in a Square Cavity with Elliptic Shape Adiabatic Block

M. Jahirul Haque Munshi^{1,*}, M. A. Alim², A. H. Bhuiyan², G. Mostafa¹

¹Department of Mathematics, Faculty of Science, Engineering & Technology
Hamdard University Bangladesh (HUB), Newtown, Sonargaon, Narayngonj-1440, Bangladesh

²Department of Mathematics, Bangladesh University of Engineering and Technology
(BUET), Dhaka- 1000, Bangladesh

ABSTRACT: In this paper, the effect of magneto-hydrodynamic natural convection fluid flow and heat transfer in a square cavity filled with an electric conductive fluid with elliptic shape adiabatic block are studied numerically. The governing differential equations are solved by using finite element method (weighted-residual method). The horizontal and top wall assumed to be adiabatic. The left wall is kept heated T_h and right wall is kept at cold T_c . Also all the walls are assumed to be no-slip condition. Numerical predictions are obtained for a wide range of Rayleigh number (Ra) and different Hartmann number (Ha) at the Prandtl number 0.733. The numerical results show that the effect of the magnetic field is to decrease the rate of convective heat transfer and the average Nusselt number decreases as Hartmann number increases. The results are presented for Rayleigh number from 10^4 up to 10^6 in form of streamlines, isotherms and Nusselt number for various Rayleigh and Hartmann numbers.

KEYWORDS: Natural convection, numerical study, square enclosure, magnetic field, elliptic shape adiabatic block.

Nomenclatures:

B_0	Strength of the magnetic field	Greek symbols	
g	gravitational acceleration	α	Thermal diffusivity
L	length of the cavity	β	Volumetric coefficient of thermal expansion
Nu	Nusselt number	ν	Kinematic viscosity of the fluid
P	dimensional pressure	θ	non-dimensional temperature
p	pressure	ρ	density of the fluid
Pr	Prandtl number	ψ	non-dimensional stream function
Ra	Rayleigh number		
T	dimensional temperature	Subscripts	
u, v	velocity components	c	cold wall
U, V	non-dimensional velocity components	h	hot wall
x, y	Cartesian coordinates		
X, Y	non-dimensional Cartesian coordinates		

I. INTRODUCTION

Natural convection is a subject of central importance in the present technology development and all kinds of engineering applications. Historically, some of the major discoveries in natural convection have helped shape the course of development and important fields for the application of the cooling of power electronics, solar collectors, solar stills, attic spaces, etc. Now a days, natural convection have industrial applications in which the heat and mass transfer occur concurrently as a result of combined buoyancy effects of thermal and species diffusion.

A number of studies have been conducted to investigate the flow and heat transfer characteristics in closed cavities in the past. Kuhen et al. (1976) an experimental and theoretical study of natural convection in the annulus between horizontal concentric cylinders. Patankar et al. (1980) Numerical methods for heat transfer and fluid flow, New York, Hemisphere. Acharya (1985) studied natural convection in an inclined enclosure containing internal energy sources and cooled from below. Fusegi et al. (1992) performed a numerical study on natural convection in a square cavity by using a high-resolution finite difference method. The authors considered differentially heated vertical walls and uniform internal heat generation in the cavity. Natural convection heat transfer in rectangular cavities heated from the bottom had been investigated by Hasaaoui et al. (1995). Ganzarolli et al. (1995) investigated the natural convection in rectangular enclosures heated from below and cooled from the sides. Turkoglu et al. (1995) made a numerical study using control volume approach for the effect of heater and cooler locations on natural convection on cavities. The authors indicated that for a given cooler position, average Nusselt number increases as the heater is moved closer to the bottom horizontal wall. Asan et al. (2000) studied the steady-state, laminar, two-dimensional natural convection in an annulus between two isothermal concentric square ducts. Roychowdhury et al. (2002) analyzed natural convective flow and heat transfer features for a heated cylinder kept in a square enclosure with different thermal boundary conditions. Dong et al. (2004) studied the conjugate of natural convection and conduction in a complicated enclosure. Their investigations showed the influences of material character, geometrical shape and Rayleigh number (Ra) on the heat transfer in the overall concerned region and concluded that the flow and heat transfer increase with the increase of thermal conductivity in the solid region; the overall flow and heat transfer were greatly affected by both geometric shape and Rayleigh number. Braga et al. (2005) numerically studied steady laminar natural convection within a square cavity filled with a fixed amount of conducting solid material consisting of either circular or square obstacles. It was found that the average Nusselt number for cylindrical rods was slightly lower than those for square rods. De et al. (2006) performed a simulation of natural convection around a tilted heated square cylinder kept in an enclosure within the range of $10^3 \leq Ra \leq 10^6$. They reported detailed flow and heat transfer features for two different thermal boundary conditions and obtained that the uniform wall temperature heating was quantitatively different from the uniform wall heat flux heating. Kahveci et al. (2007) studied natural convection in a partitioned vertical enclosure heated with a uniform heat flux. Basak et al. (2008) studied and solved the finite element analysis of natural convection flow in a isosceles triangular enclosure due to uniform and non-uniform heating at the side walls. Pirmohammadi et al. (2009) shows that the effect of a magnetic field on Buoyancy- Driven convection in differentially heated square cavity.

Rahman et al. (2011) offered a numerical model for the simulation of double-diffusive natural convection in a right-angled triangular solar collector. Mahmoodi et al. (2011) studied numerically magneto-hydrodynamic free convection heat transfer in a square enclosure heated from side and cooled from the ceiling. Jani et al. (2013) numerically investigated magneto-hydrodynamic free convection in a square cavity heated from below and cooled from other walls. Bhuiyan et al. (2014) numerically investigated magneto hydrodynamic free convection in a square cavity with semicircular heated block.

On the basis of the literature review, it appears that no work was reported on the natural convection flow in a square cavity with elliptic shape adiabatic block. The obtained numerical results are presented graphically in terms of streamlines, isotherms, local Nusselt number and average Nusselt number for different Hartmann numbers and Rayleigh numbers.

II. PHYSICAL CONFIGURATION

The physical model considered in the present study of natural convection in a square enclosure with elliptic shape adiabatic block is shown in Fig. 1.

The height and the width of the cavity are denoted by L and inside the cavity with elliptic shape adiabatic block. The left wall is kept heated T_h and right wall is kept at cold T_c . The magnetic field of strength B_0 is applied parallel to x - axis. The square cavity is filled with an electric conductive fluid with $Pr = 0.733$ that is considered Newtonian and incompressible.

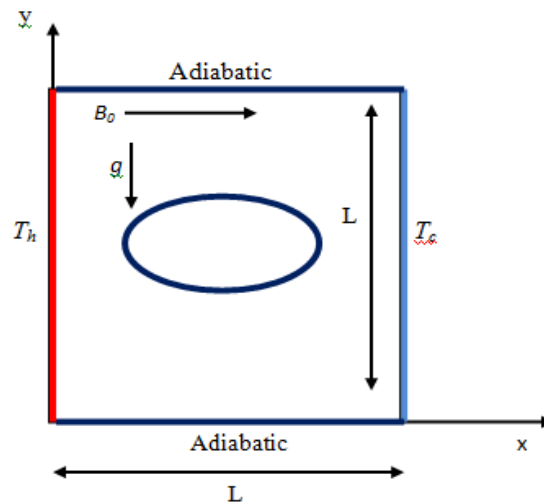


Fig. 1

Fig. 1. Schematic view of the cavity with boundary conditions considered in the present paper

III. MATHEMATICAL FORMULATION

The flow is considered to be two dimensional, steady, laminar and incompressible fluids. The governing equations for mass, momentum and energy equation and natural convection flow in a cavity are as follows:

$$\frac{\partial u}{\partial x} + \frac{\partial v}{\partial y} = 0 \tag{1}$$

$$\rho \left(\frac{\partial u}{\partial x} + \frac{\partial u}{\partial y} \right) = -\frac{\partial p}{\partial x} + \mu \left(\frac{\partial^2 u}{\partial x^2} + \frac{\partial^2 u}{\partial y^2} \right) \tag{2}$$

$$\rho \left(\frac{\partial v}{\partial x} + \frac{\partial v}{\partial y} \right) = -\frac{\partial p}{\partial y} + \mu \left(\frac{\partial^2 v}{\partial x^2} + \frac{\partial^2 v}{\partial y^2} \right) + \rho g \beta (T - T_c) - \sigma B_0^2 v \tag{3}$$

$$u \frac{\partial T}{\partial x} + v \frac{\partial T}{\partial y} = \alpha \left(\frac{\partial^2 T}{\partial x^2} + \frac{\partial^2 T}{\partial y^2} \right)$$

where x and y are the distances measured along the horizontal and vertical directions respectively, u and v are the velocity components in the x and y directions respectively, T denotes the fluid temperature, p is the pressure and ρ is the fluid density.

Boundary conditions:

On the left wall of the square cavity: $u = 0, v = 0, T = T_h$

On the right wall of the square cavity: $u = 0, v = 0, T = T_c$

The above equations are non-dimensionalized by using the following dimensionless quantities

$$X = \frac{x}{L}, Y = \frac{y}{L}, U = \frac{uL}{\alpha}, V = \frac{vL}{\alpha}, P = \frac{pL^2}{\rho\alpha^2}, \theta = \frac{(T - T_c)}{(T_h - T_c)} \tag{5}$$

where $\nu = \frac{\mu}{\rho}$ is the reference kinematic viscosity and θ is the non-dimensional temperature. After substitution of dimensionless variable we get the non-dimensional governing equations which are:

$$\frac{\partial U}{\partial X} + \frac{\partial V}{\partial Y} = 0 \tag{6}$$

$$U \frac{\partial U}{\partial X} + V \frac{\partial U}{\partial Y} = -\frac{\partial P}{\partial X} + \text{Pr} \left(\frac{\partial^2 U}{\partial X^2} + \frac{\partial^2 U}{\partial Y^2} \right) \tag{7}$$

$$\rho \left(\frac{\partial v}{\partial x} + \frac{\partial v}{\partial y} \right) = -\frac{\partial p}{\partial y} + \mu \left(\frac{\partial^2 v}{\partial x^2} + \frac{\partial^2 v}{\partial y^2} \right) + \rho g \beta (T - T_c) - \sigma B_0^2 v \tag{8}$$

$$U \frac{\partial \theta}{\partial X} + V \frac{\partial \theta}{\partial Y} = \left(\frac{\partial^2 \theta}{\partial X^2} + \frac{\partial^2 \theta}{\partial Y^2} \right) \tag{9}$$

where Ra , Pr and Ha are the Rayleigh, Prandtl and Hartman numbers are defined as follows:

$$Ra = \frac{g\beta(T_h - T_c)L^3}{\alpha\nu}, \text{Pr} = \frac{\nu}{\alpha}, Ha = B_0L \sqrt{\frac{\sigma}{\rho\nu}} \tag{10}$$

where g is the gravitational acceleration, ν is the dynamic viscosity, β is the volumetric coefficient of thermal expansion, B_0 is the magnitude of magnetic field, α is the thermal diffusivity.

The effect of magnetic field into the momentum equation is introduced through the Lorentz force term $\vec{j} \times \vec{B}$ that is reduced to $-\sigma B_0 v^2$ as shown by Pirmohammadi et al. (2009).

To computation of the rate of heat transfer, Nusselt number along the hot wall of the enclosure is used as follows:

$$Nu_y = \frac{\frac{\partial \theta}{\partial X}|_{X=0}}{(\theta_h - \theta_c)} \quad Nu_x = \int_0^1 Nu_y dY \tag{11}$$

Boundary conditions:

On the left wall of the square cavity: $U = 0, V = 0, \theta = 1$

On the right wall of the square cavity: $U = 0, V = 0, \theta = 0$

The non-dimensional stream function is defined as $U = \frac{\partial \psi}{\partial Y}, V = -\frac{\partial \psi}{\partial X}$ (12)

IV. NUMERICAL TECHNIQUE

The nonlinear governing partial differential equations, i.e., mass, momentum and energy equations are transferred into a system of integral equations by using the Galerkin weighted residual finite-element method. The integration involved in each term of these equations is performed with the aid Gauss quadrature method. The nonlinear algebraic equations so obtained are modified by imposition of boundary conditions. These modified nonlinear equations are transferred into linear algebraic equations with the aid of Newton’s method. Lastly, Triangular factorization method is applied for solving those linear equations.

4.1. Program Validation and Comparison with Previous Work

In order to check on the accuracy of the numerical technique employed for the solution of the problem considered in the present study, the code is validated with Pirmohammadi et al. (2009). The left wall is kept heated T_h and right wall is kept at cold T_c . By performing simulation for natural convection in the upper and lower wall are adiabatic. Streamlines and isotherms are plotted in Fig. 2. showing good agreement.

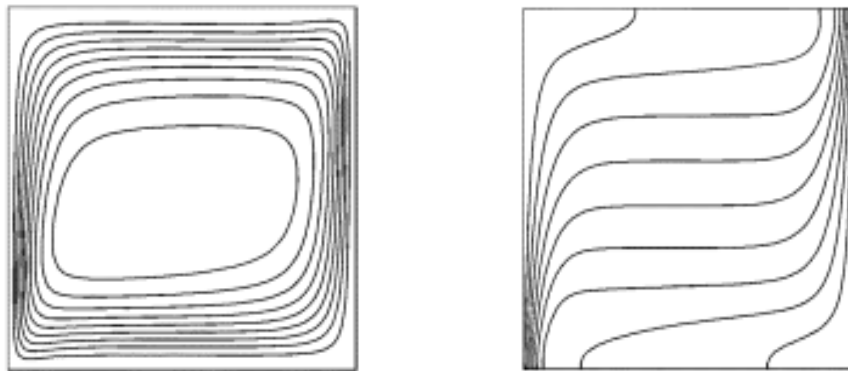


Fig. 2(a). Pirmohammadi et al. [15] Obtained streamlines and Isotherms for $Ra = 10^6$, $Pr = 0.733$ and $Ha=50$.

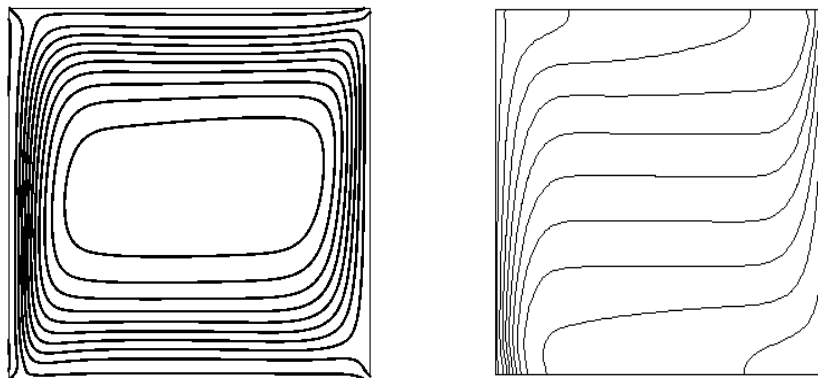


Fig. 2(b). Present: Obtained streamlines and Isotherms for $Ra = 10^6$, $Pr = 0.733$ and $Ha = 50$

V. RESULT AND DISCUSSION

A numerical work was performed by using finite element method to natural convection in a square enclosure with elliptic shape adiabatic block. In this section, some representative results are presented to illustrate the effects of various controlling parameters on the fluid flow and heat transfer processes inside the cavity. These controlling parameters include Rayleigh number ranging from 10^4 to 10^6 and the Hartmann number varying from 0 to 150 with fixed Prandtl number $Pr = 0.733$. The results are presented in terms of streamlines and isotherms inside the cavity at various Hartmann numbers and Rayleigh numbers is shown in Figs. 3, 4, 5 and 6, 7, 8. The maximum absolute value of stream function can be viewed as a measure of the intensity of natural convection in the cavity. It is evident from the Figs. 3 to 8 that because of the absent of magnetic field, the maximum value of the stream function increases due to the increase of the Hartmann number.

We observed from the figures with existence centerline of the cavity, the flow and temperature fields are symmetrical about this line. As can be seen from the streamlines in the Fig. 3, 4, 5 a pair of counter-rotating eddies are formed in the left and right half of the cavity for all Rayleigh numbers considered. Each cell ascend through the symmetry axis, then faces the right wall and moves horizontally and finally descends along the corresponding cold side wall. Since upper, lower walls adiabatic and elliptic shape adiabatic block, so the curve moves to left wall to right wall.

From this figure we see that, as the Hartmann number increases 100 to 150, the central stream line is elongated. The isotherms are shown almost parallel to the vertical walls, indicating that most of the heat transfer is by heat conduction. The main effect of the introduction of the magnetic field is to decrease the overall heat transfer rate between the hot and cold walls. For moderate and high Rayleigh numbers 10^5 to 10^6 and for a weak magnetic field strength there is a temperature stratification in the vertical direction and the thermal boundary layer is wall established along the side walls. This is because at high Rayleigh number and low Hartmann number, convection is dominant heat transfer mechanism. Heat transfer by convection alters the temperature distribution to such an extent that temperature gradients in the centre is closed to zero. From the stream line pattern we see that there is a strong upward flow near the heated side wall and downward flow at the cold wall. With increases in Rayleigh number and buoyancy force, the elliptic shape of the eddies move upward in so far as at $Ra = 10^6$, locate in the upper half of the cavity. At $Ra = 10^6$ the elliptic shape are elongated along the height of the cavity.

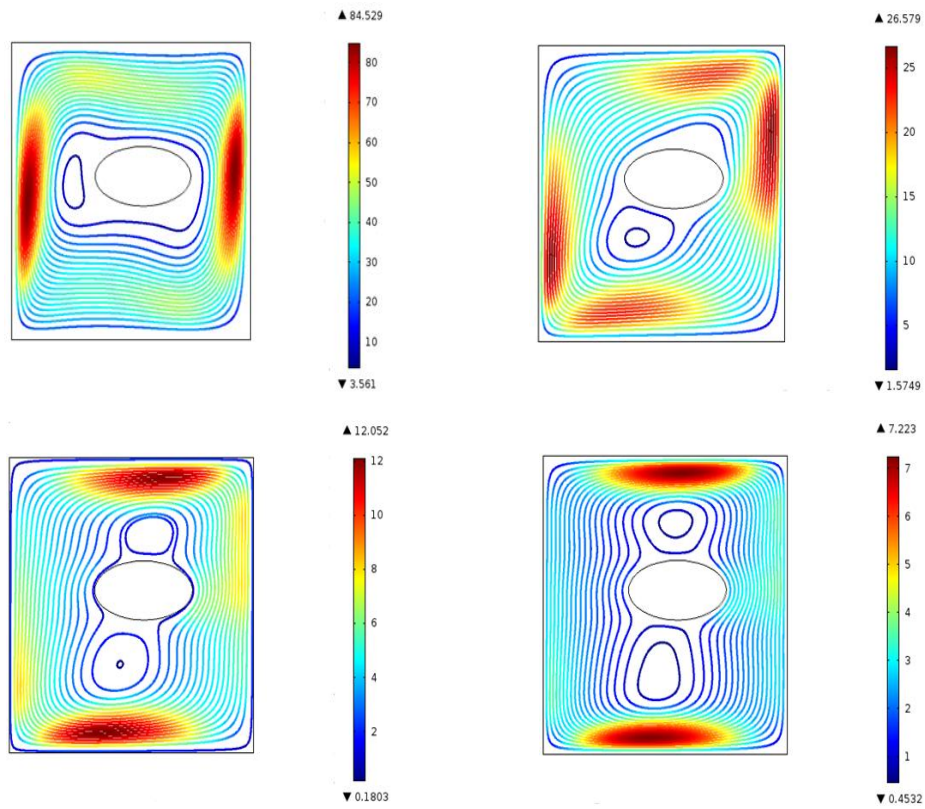


Fig. 3. Streamlines for (a) $Ha = 0$; (b) $Ha = 50$; (c) $Ha = 100$; (d) $Ha = 150$ while $Ra = 10000$ and $Pr = 0.733$

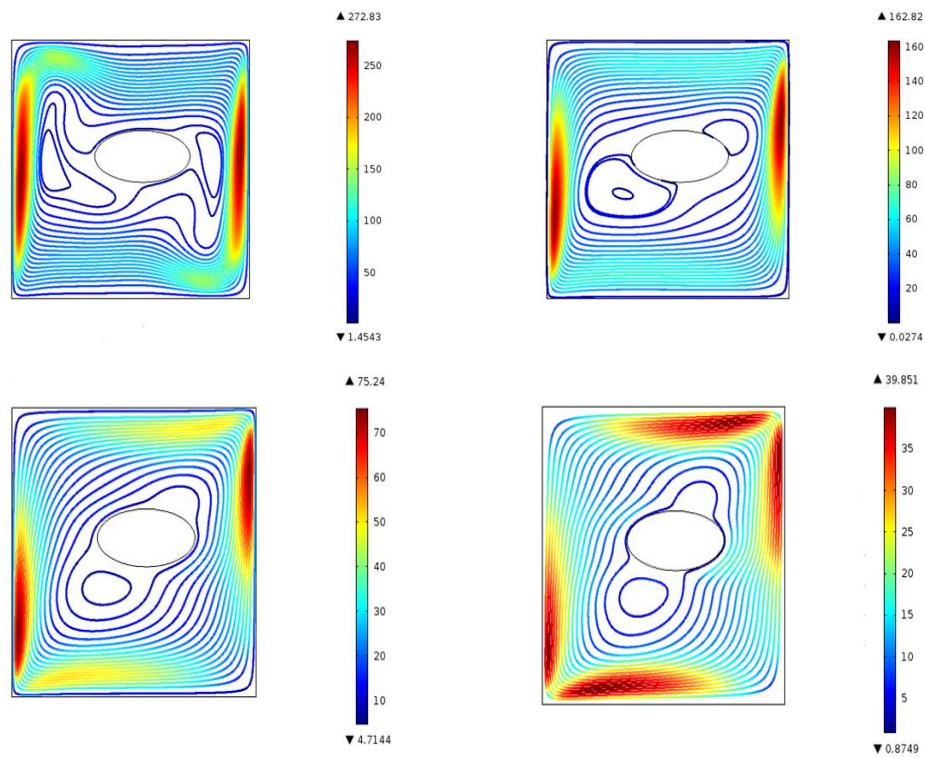


Fig. 4. Streamlines for (a) $Ha = 0$; (b) $Ha = 50$; (c) $Ha = 100$; (d) $Ha = 150$ while $Ra = 100000$ and $Pr = 0.733$

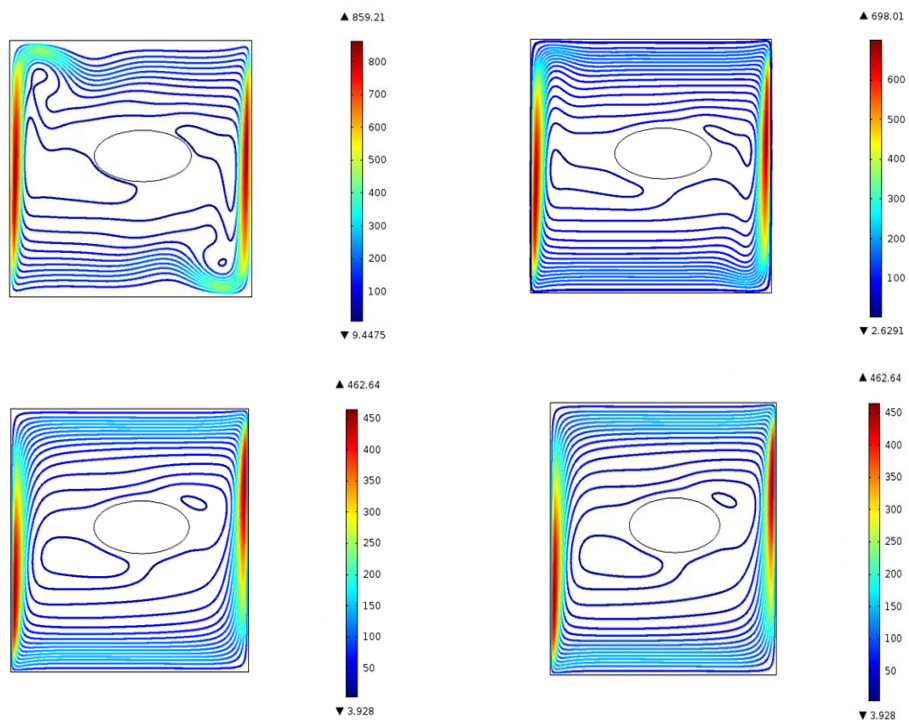


Fig. 5. Streamlines for (a) $Ha = 0$; (b) $Ha = 50$; (c) $Ha = 100$; (d) $Ha = 150$ while $Ra = 1000000$ and $Pr = 0.733$

Conduction dominant heat transfer is observed from the isotherms in Fig. 6, 7, 8 at $Ra = 10^4$ to 10^6 . With increasing the Rayleigh number, the isotherms are condensed next to the side wall which means increasing heat transfer through convection. Formation of thermal boundary layers can be found from the isotherms at $Ra = 10^4$ and 10^6 . The cavity was heated at the left and right wall are cooled while the rest of the boundaries were insulated.

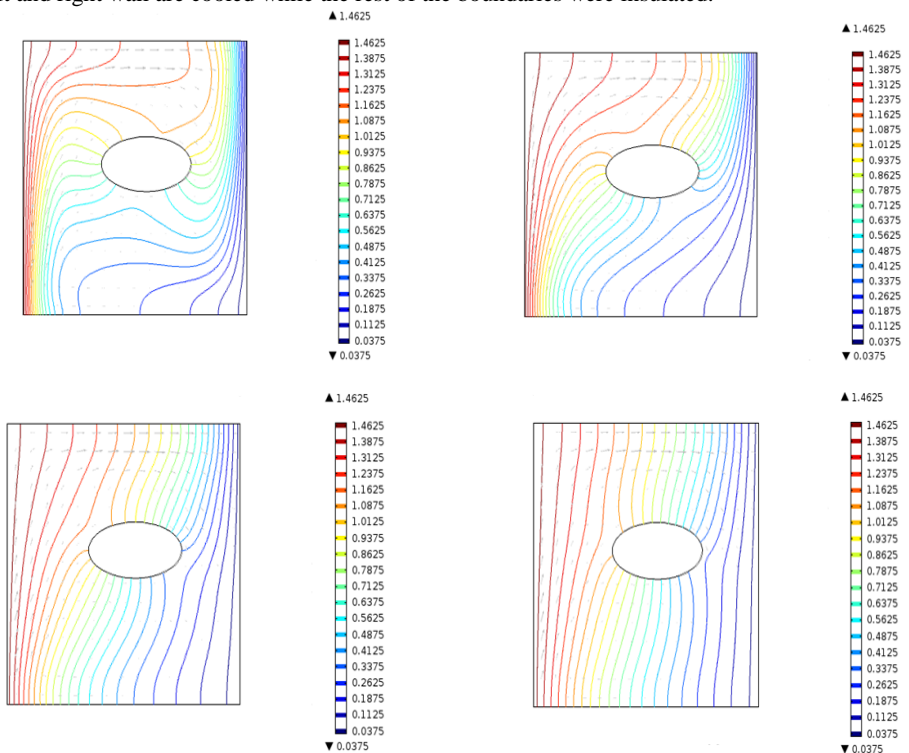


Fig. 6. Isotherms for (a) $Ha = 0$; (b) $Ha = 50$; (c) $Ha = 100$; (d) $Ha = 150$ while $Ra = 10000$ and $Pr = 0.733$

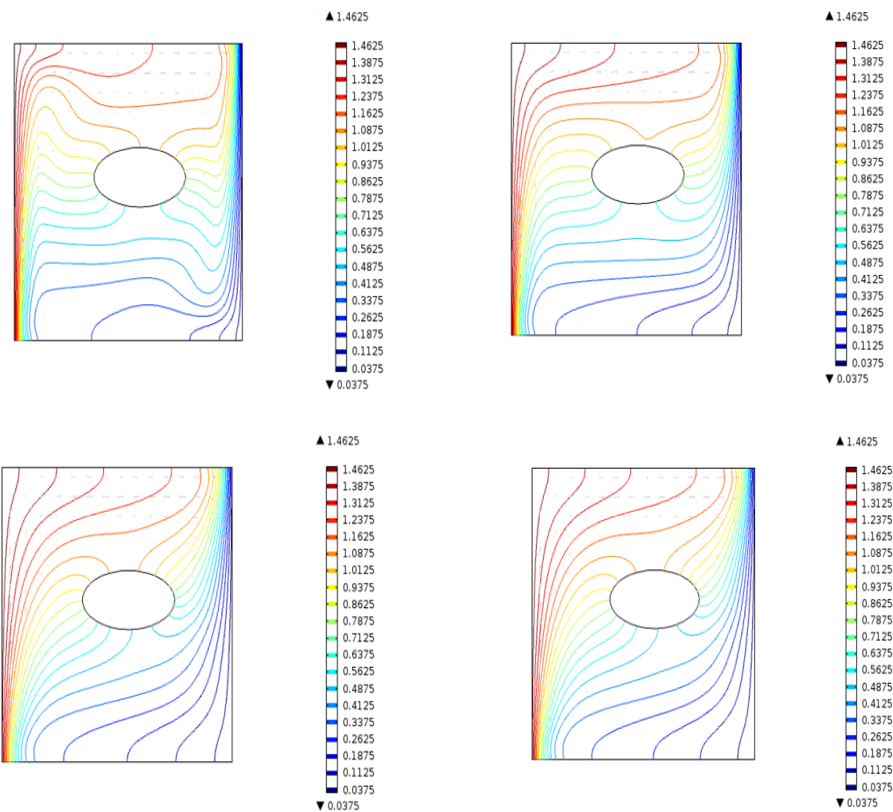


Fig. 7. Isotherms for (a) $Ha = 0$; (b) $Ha = 50$; (c) $Ha = 100$; (d) $Ha = 150$ while $Ra = 100000$ and $Pr = 0.733$.

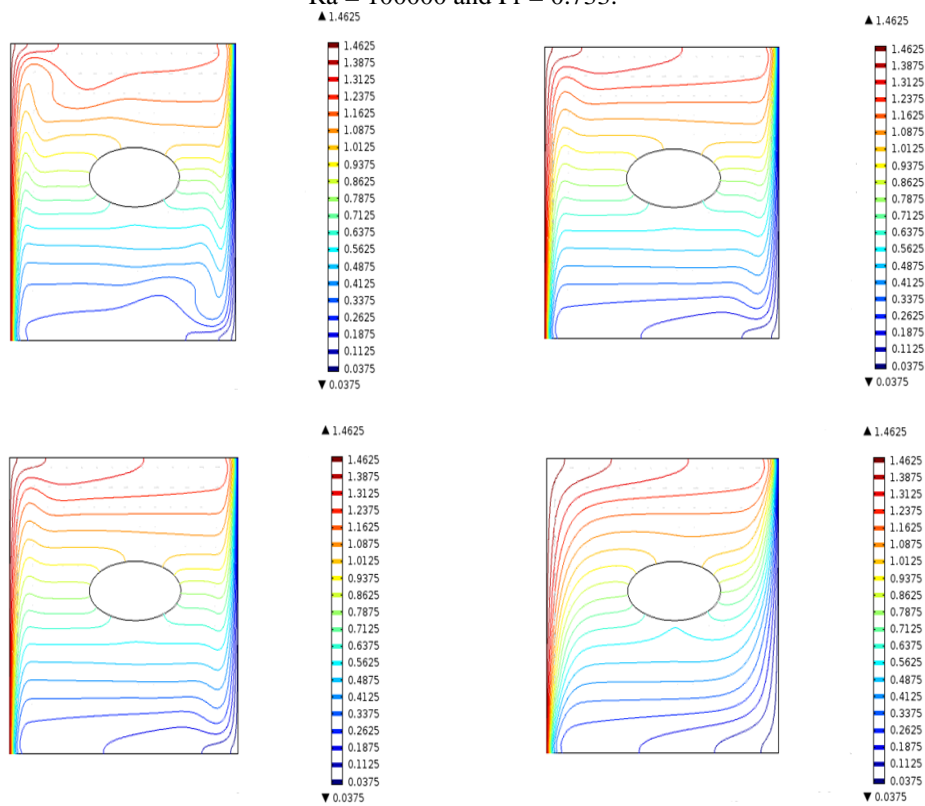


Fig. 8. Isotherms for (a) $Ha = 0$; (b) $Ha = 50$; (c) $Ha = 100$; (d) $Ha = 150$ while $Ra = 1000000$ and $Pr = 0.733$

Variations of the local Nusselt number along the bottom wall of the square cavity with the Rayleigh number at different Hartmann number shown in Fig. 9. Owing to the symmetry in thermal boundary conditions, the local Nusselt number is symmetrical with respect to the vertical midline of the cavity. We see from the figure that the local Nusselt number increases with the Rayleigh number in major portion of the hot wall. In the middle of the bottom wall the local Nusselt number equals to zero and does not change significantly with increase in the Rayleigh number. It can be seen from the figure that the local Nusselt number increases with the Rayleigh number in major portion of the hot wall. In the middle of the left wall the local Nusselt number equals to zero and does not change significantly with increase in the Hartmann number.

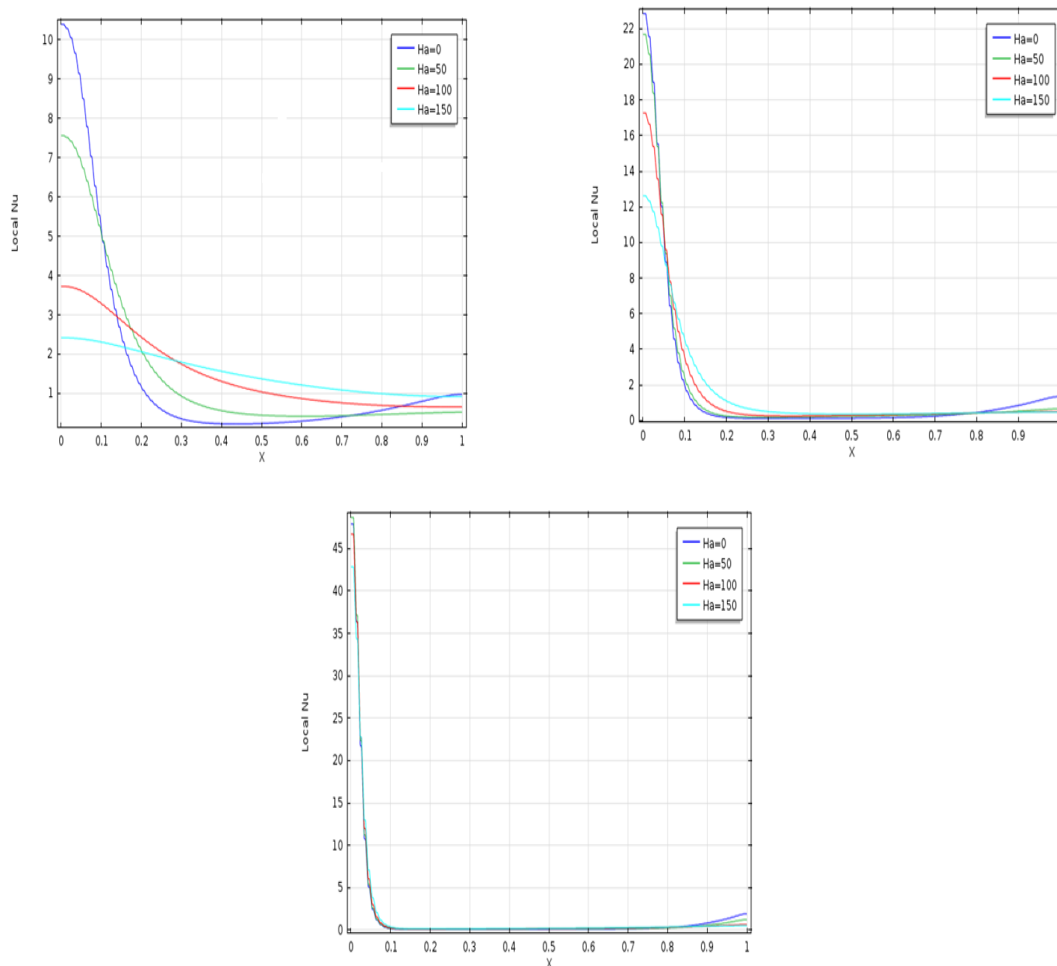


Fig. 9. Variation of local Nusselt number along the bottom wall for different Hartmann number with $Pr = 0.733$ and $Ra = Ra = 10000, 100000, 1000000$.

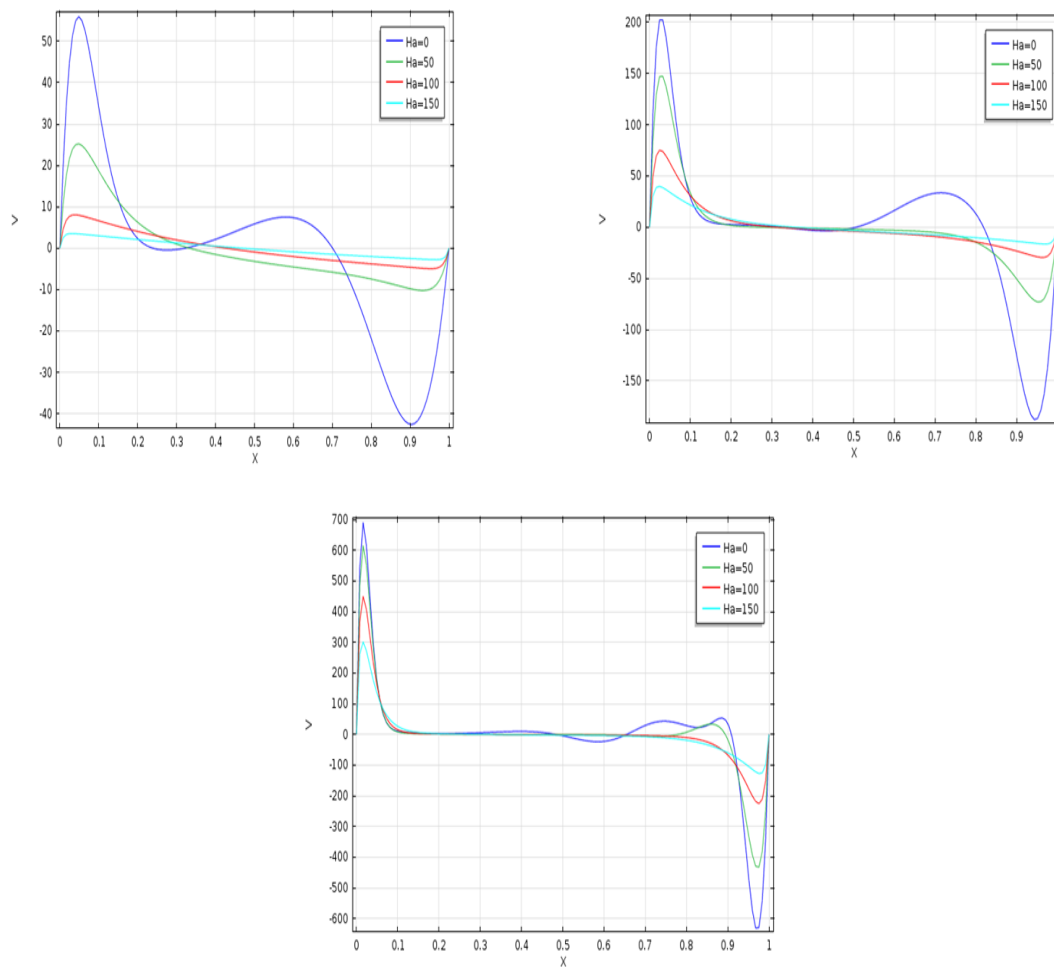


Fig. 10. Variation of velocity profile along the bottom wall at different Hartmann number with $Pr = 1.733$ and $Ra = 10000, 100000, 1000000$

Variations of the velocity components along the bottom wall for different Rayleigh number with $Pr = 0.733$ of the cavity are shown in Fig. 10. From the figure it can be observed that the curves are symmetrical x -axis because of symmetrical adiabatic ellipse block. The velocity increasing and decreasing for various types of Rayleigh number when $Ha = 0$.

Variation of the dimensionless temperature along the bottom wall of the square cavity with Rayleigh number at different Hartmann number are shown in Fig. 11. For moderate and high Rayleigh number ($Ra = 10^4, 10^5$ and 10^6) and for a weak magnetic field strength there is a temperature of the absolute value of maximum and minimum value of temperature increases with increasing the Rayleigh number (increasing the buoyant force). Convection is dominant heat transfer mechanism because of high Ra and low Ha . Heat transfer by convection alters the temperature distribution to such an extent that temperature gradients in the centre are close to zero. From the stream line pattern we see that there is a strong upward flow near the cold wall and downward flow at the hot wall.

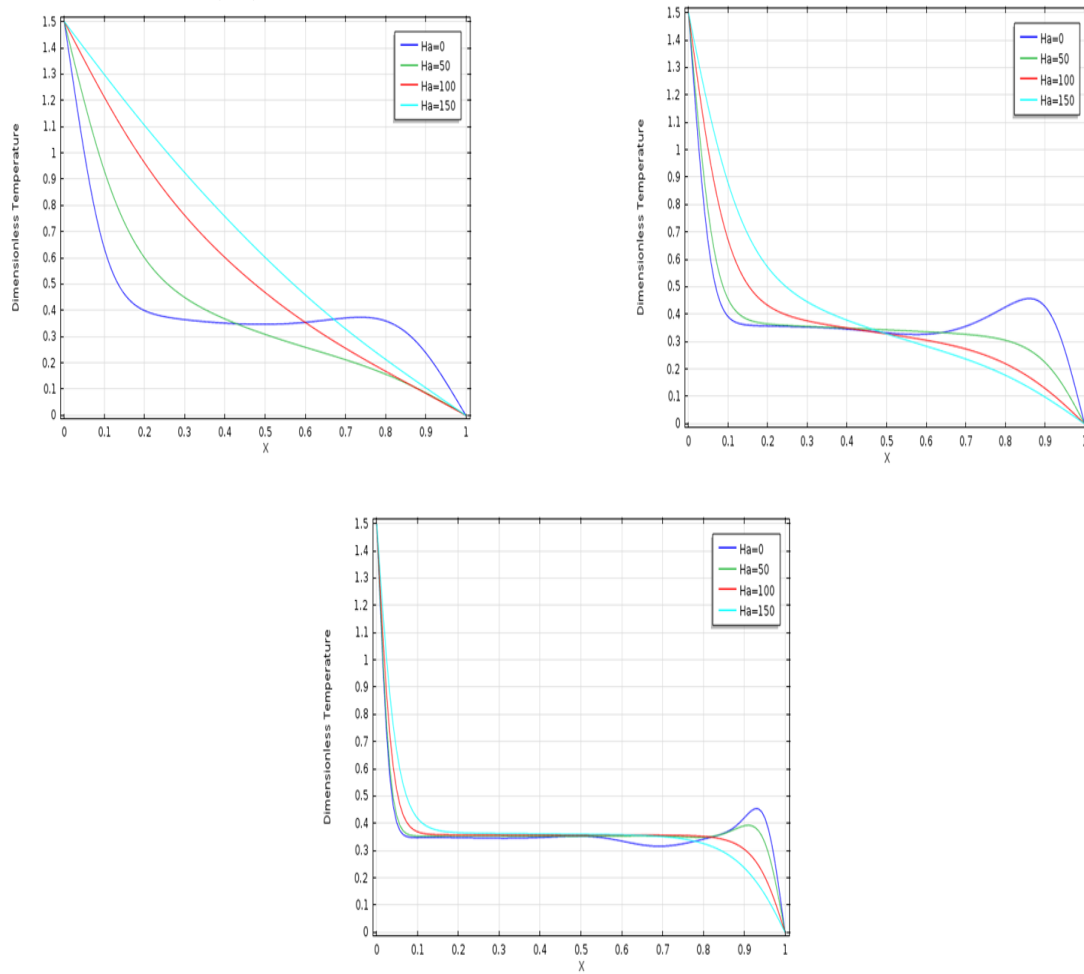
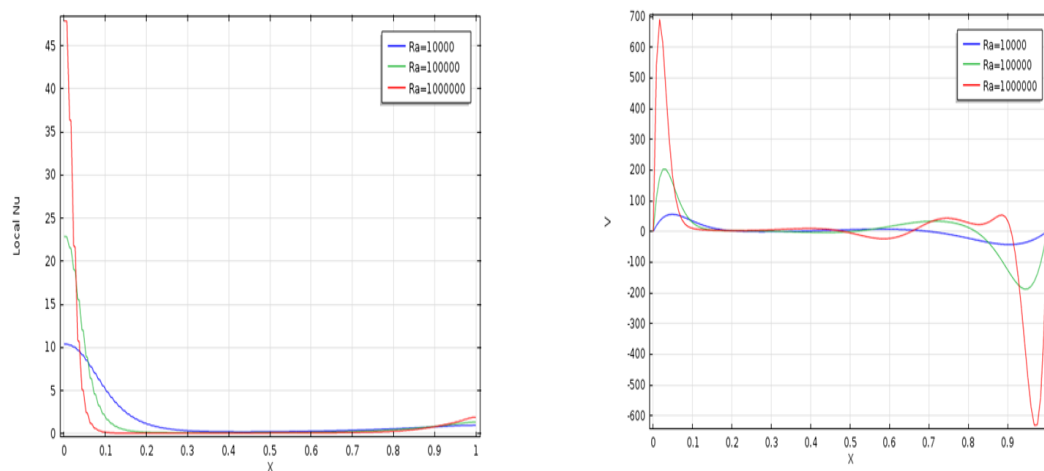


Fig. 11. Variation of temperature profiles along the bottom wall at different Hartmann number with $Pr = 1.733$ and $Ra = 10000, 100000, 1000000$.

Also effect of different Rayleigh numbers on the flow field while $Ha = 0$ and $Pr = 0.733$ are shown in figure below. Variation of local Nusselt number, Variation of velocity profiles, Variation of dimensionless temperature profiles, and Variation of the average Nusselt number are shown below in Fig. 12.



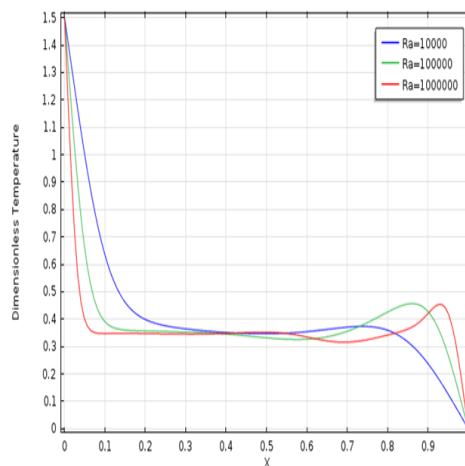


Fig. 12. Variation of local Nusselt number, velocity profile, temperature profiles along the bottom wall at different Rayleigh number with $Pr = 0.733$ and $Ha = 0$.

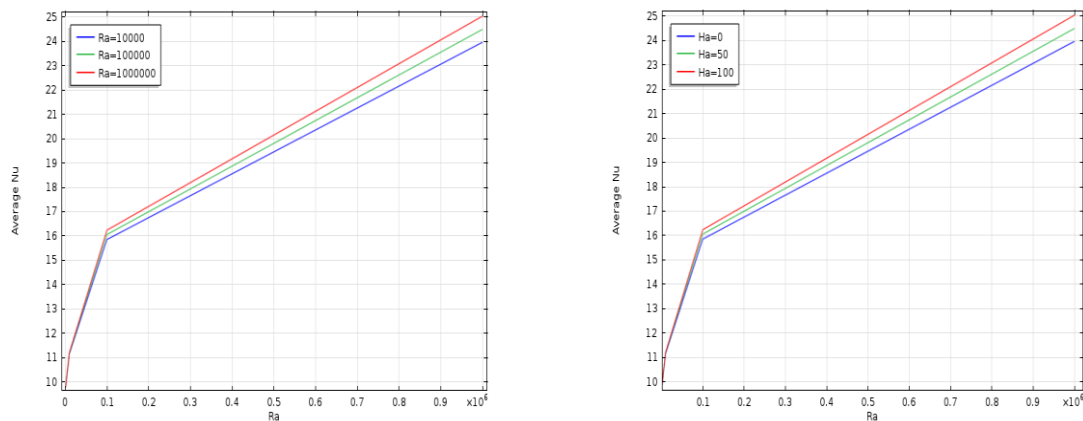


Fig. 13. Variation of the average Nusselt number along the bottom wall of the square cavity with different Rayleigh numbers & different Hartmann numbers at Prandtl number 0.733.

Plot of the average Nusselt number of the adiabatic bottom wall as a function of Rayleigh number at different Hartmann number is shown in Fig. 13. For a fixed Hartmann number, with increases in the Prandtl number the flow velocity decreases, the free convection is suppressed and finally the rate of heat transfer decreases. When Ra increases then we see that the flow strength is also increases in cold & adiabatic walls at fixed Ha & Pr . At a constant Prandtl number, with increase in Rayleigh number the buoyancy force increases and the heat transfer is enhanced. Therefore at high Rayleigh numbers, a relatively stronger magnetic field is needed to decrease the rate of heat transfer.

VI. CONCLUSION

Effect of magneto-hydrodynamic natural convection fluid flow and heat transfer in a square cavity filled with an electric conductive fluid with elliptic shape adiabatic block are studied numerically. Finite element method was used to solve governing equations for a heat generation parameters, Rayleigh numbers and Hartmann numbers. We observed that there were very good agreements between Ra & Ha in different cases. For all cases considered, two counter rotating eddies were formed inside the cavity regardless the Rayleigh and the Hartmann numbers. The obtained results showed that the heat transfer mechanisms, temperature distribution and the flow characteristics inside the cavity depended strongly upon both the strength of the magnetic field and the Rayleigh numbers. From the present investigation the following conclusions may be drawn as: with increase in the buoyancy force via increase in Rayleigh number, to decrease natural convection, a stronger magnetic field is needed compared to the lower Rayleigh numbers.

REFERENCES

- [1] T.H. Kuhen, R.J. Goldstein (1976): an experimental and theoretical study of natural convection in the annulus between horizontal concentric cylinders, *J. of Fluid Mechanics*, vol. 74, pp. 695- 719.
- [2] S. V. Patankar (1980): *Numerical methods for heat transfer and fluid flow*, New York, Hemisphere.
- [3] Acharya, S. (1985): Natural convection in an inclined enclosure containing internal energy sources and cooled from below, *Int. J. Heat & Fluid flow*, vol. 6, No. 2, pp. 113-121. doi:10.1016/0142-727X(85)90045-1.
- [4] Fusegi, T., Hyun, J. M., Kuwahara, K. (1992): Natural convection in a differentially Heated square cavity with internal heat generation, *Num. Heat Transfer Part A*, vol. 21, pp. 215-229. doi:10.1080/10407789108944873.
- [5] Hasnaoui, M., Bilgen, E., Vasseur, P. (1995): Natural convection heat transfer in rectangular cavities heated from below, *J. Thermophysics Heat Transfer*, vol.6, pp. 225-264.
- [6] Ganzaroli, M., M., Milanez, L., F. (1995): Natural convection in rectangular enclosures heated from below and symmetrical cooled from the sides, *Int. J. of Heat and Mass Transfer*, vol. 38, pp.1063-1073. doi:10.1016/0017-9310(94)00217-J.
- [7] Turkoglu, H., Yucel, N. (1995): Effect of heater and cooler locations on ural convection in square cavities, *Num. Heat Transfer Part A*, vol. 27, pp. 351-358. doi:10.1080/10407789508913705
- [8] H. Asan (2000): Natural convection in an annulus between two isothermal concentric square ducts, *Int. Comm. Heat Mass Transfer*, vol. 27, pp. 367-376.
- [9] D. G. Roychowdhury, S. K. Das, and T. S. Sundararajan.(2002): Numerical Simulation of Natural Convection Heat Transfer and Fluid Flow Around a Heated Cylinder Inside an Enclosure, *Heat Mass Transfer*, vol. 38, pp. 565- 576.
- [10] S. F. Dong and Y. T. Li.(2004): Conjugate of Natural Convection and Conduction in a Complicated Enclosure, *Int. J. Heat Mass Transfer*, vol. 47, pp. 2233- 2239.
- [11] E. J. Braga and M. J. S. de Lemos.(2005): Laminar Natural Convection in Cavities Filled with Circular and Square Rods, *Int. Comm. Heat Mass Transfer*, vol. 32, pp. 1289- 1297.
- [12] A. K. De and A. Dalal.(2006): A Numerical Study of Natural Convection Around a Square Horizontal, Heated Cylinder Placed in an Enclosure, *Int. J. Heat Mass Transfer*, vol. 49, pp. 4608- 4623.
- [13] K. Kahveci, (2007): Natural convection in a partitioned vertical enclosure heated with a uniform heat flux, *J. Heat Transfer*, vol. 129, pp. 717-726.
- [14] T. Basak, S. Roy, S.K. Babu, A.R. Balakrishnan, (2008): Finite element analysis of natural convection flow in a isosceles triangular enclosure due to uniform and non- uniform heating at the side walls, *Int. J. Heat Mass Transfer*, vol. 51, pp. 4496-4505.
- [15] Mohsen Pirmohammadi, Majid Ghassemi, and Ghanbar Ali Sheikhzadeh, (2009): Effect of a magnetic field on Buoyancy-Driven convection in differentially heated square cavity, *IEEE transactions on magnetic*, Vol. 45, No. 1.
- [16] M.M. Rahman, M.M. Billah, N. A. Rahim, N. Amin, R. Saidur and M. Hasanuzzaman,(2011): A numerical model for the simulation of double-diffusive natural convection in a right-angled triangular solar collector, *International Journal of Renewable Energy Research* 1(50-54).
- [17] M. Mahmoodi, Z. Talea'pour, (2011): 'Magnetohydrodynamic Free Convection Heat Transfer in a Square Enclosure heated from side and cooled from the ceiling' *Computational Thermal Science*, vol. 3, 219- 226.
- [18] S. Jani, M. Mahmoodi, M. Amini, (2013): Magnetohydrodynamic free convection in a square cavity heated from below and cooled from other walls, *International Journal of Mechanical, Industrial Science and Engineering* Vol. 7 No. 4.
- [19] A. H. Bhuiyan, R. Islam, M. A. Alim, (2014): Magnetohydrodynamic free convection in a square cavity with semicircular heated block, *International Journal of Engineering Research & Technology (IJERT)*, Vol. 3 Issue 11.